Title: Data to support The Effect of Inert Dopant Ions on Spin-Crossover Materials is not Simply Controlled by Chemical Pressure

Creator(s): Prabir Ghosh,[1] Christopher M. Pask,[2] Hari Babu Vasili,[2] Nobuto Yoshinari,[3] Takumi Konno,[3,4] Oscar Cespedes,[2] Cristian Enachescu,[5] Pradip Chakraborty[1] and Malcolm A. Halcrow[2]

Organisation(s): 1. IIT Kharagpur, India. 2. University of Leeds, UK. 3. Osaka University, Japan. 4. Current address: National Taiwan Normal University, Taiwan. 5. Alexandru Ioan Cuza University, Romania.

Publication Year: 2023

Description: Different compositions of doped materials $[Fe_zZn_{1-z}(bpp)_2][BF_4]_2$ and $[Fe_zRu_{1-z}(bpp)_2][BF_4]_2$ show similar broadening of the SCO transition with increased doping, but differ in their effect on the transition temperature. Doping with zinc strongly lowers $T_{½}$, which is consistent with previous work. In contrast, doping with ruthenium increases $T_{½}$ to a smaller degree, which cannot be explained by the chemical pressure arguments that are conventionally applied to doped SCO materials. Simulations using a mechanoelastic model imply these results can be explained, if elastic interactions between nearest neighbour iron and dopant centres in the lattice depend on the identity of the dopant. Crystallographic data rationalize this by implying the molecular structure of high-spin $[Fe(bpp)_2]^{2+}$ is influenced by the presence of different dopant molecules.

Cite as: Ghosh, Prabir, Pask, Christopher M., Vasili, Hari Babu, Yoshinari, Nobuto, Konno, Takumi, Cespedes, Oscar, Enachescu, Cristian, Chakraborty, Pradip, and Halcrow, Malcolm A. (2023). Data to support The Effect of Inert Dopant Ions on Spin-Crossover Materials is not Simply Controlled by Chemical Pressure. University of Leeds. [Dataset] https://doi.org/10.5518/1351

Related publication: Ghosh, Prabir, Pask, Christopher M., Vasili, Hari Babu, Yoshinari, Nobuto, Konno, Takumi, Cespedes, Oscar, Enachescu, Cristian, Chakraborty, Pradip, and Halcrow, Malcolm A. (2023). The Effect of Inert Dopant Ions on Spin-Crossover Materials is not Simply Controlled by Chemical Pressure. *Journal of Materials Chemistry C*, doi: 10.1039/d3tc02683c.

Contact: m.a.halcrow@leeds.ac.uk

2. TERMS OF USE

3. PROJECT AND FUNDING INFORMATION

Title: Elucidating Fundamental Mechanisms in Switchable Molecular Materials
Dates: 2020-2022
Funding organisation: The Royal Society (UK)
Grant no.: IES\R3\193172

Title: Metallo-Supramolecular and Functional Complexes
Dates: 2021-2023
Funding organisation: Diamond Light Source (UK)
Grant no.: CY26879

Title: Synthesis, Design and Stimuli-responsive Functionalities in Switchable Inorganic Materials: From Bulk to Single Molecule
Dates: 2019-2022
Funding organisation: Science and Engineering Research Board (India)
Grant no.: ECR/2018/000923

Title: n/a
Dates: n/a
Funding organisation: Science and Engineering Research Board (India)
Grant no.: PDF/2021/004430

Title: Studies on Dynamic Phenomena in Nanomaterials with Spin Transition
Dates: 2021-2023
Funding organisation: UEFISCDI (Romania)
Grant no.: PN-III-P4-ID-PCE-2020-1946

4. CONTENTS

The dataset contains data for this study:

Elemental microanalyses (*microanalysis.zip*).

X-ray powder diffraction data (measured and simulated – *XRPD*.zip).

Solid state magnetic susceptibility measurements (raw and processed data – *SQUID*.zip).

X-ray Crystallographic data (*crystal*.zip):

- Structure of **1c** at 300 K (CCDC 2261786)
- Structure of **1c** at 100 K, ordered cation refinement (CCDC 2261787)
- Structure of **1c** at 100 K, disordered cation refinement (CCDC 2261788)
- Structure of **2c** at 350 K (CCDC 2261789)
- Structure of **2c** at 200 K (CCDC 2261790)
- Structure of **2c** at 100 K, ordered cation refinement (CCDC 2261791)
- Structure of **2c** at 100 K, disordered cation refinement (CCDC 2261792)
- Structure of **3c** at 350 K (CCDC 2261793)
- Structure of **3c** at 200 K (CCDC 2261794)
- Structure of **3c** at 100 K, ordered cation refinement (CCDC 2261795)
- Structure of **3c** at 100 K, disordered cation refinement (CCDC 2261796)
- Variable temperature unit cell data for **1c**
- Variable temperature unit cell data for **2c**
- Variable temperature unit cell data for **3c**
- Variable temperature unit cell data for $[Fe(bpp)_2][BF_4]_2$
- Variable temperature unit cell data for $[Zn(bpp)_2][BF_4]_2$
- Variable temperature unit cell data for $[Ni(bpp)_2][BF_4]_2$
- Variable temperature unit cell data for $[Ru(bpp)_2][BF_4]_2$

Linear thermal expansion coefficient calculations (*PASCal* outputs – *LTE*.zip)

Differential Scanning Calorimetry data (*DSC*.zip).

The mechanoelastic model simulation data in the study belong to Dr. Cristian Enachescu (Alexandru Ioan Cuza University, Romania; cristian.enachescu@uaic.ro). Please contact him for details.

5. METHODS

Full details are provided in the related publication, listed above.

Compounds referred to in this dataset

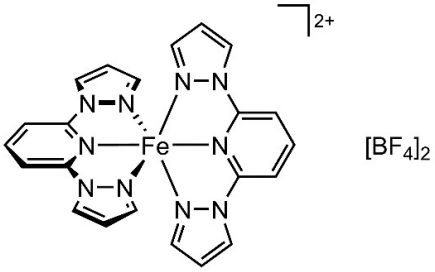

$[Fe(bpp)_2][BF_4]_2$
Bis[di(pyrazol-1-yl)pyridine]iron(II) di(tetrafluoroborate)
$C_{22}H_{18}B_2F_8FeN_{10}$

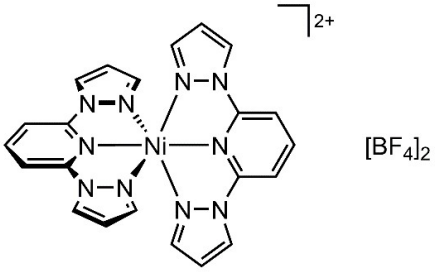

$[Ni(bpp)_2][BF_4]_2$
Bis[di(pyrazol-1-yl)pyridine]nickel(II) di(tetrafluoroborate)
$C_{22}H_{18}B_2F_8N_{10}Ni$

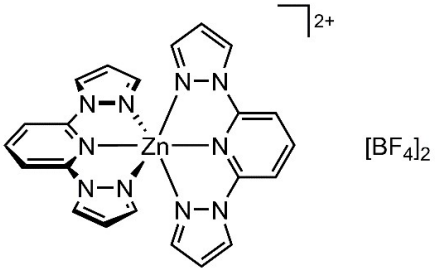

$[Zn(bpp)_2][BF_4]_2$
Bis[di(pyrazol-1-yl)pyridine]zinc(II) di(tetrafluoroborate)
$C_{22}H_{18}B_2F_8N_{10}Zn$

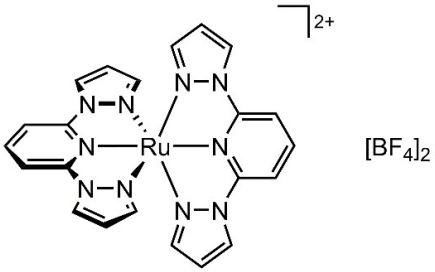

$[Ru(bpp)_2][BF_4]_2$
Bis[di(pyrazol-1-yl)pyridine]ruthenium(II) di(tetrafluoroborate)
$C_{22}H_{18}B_2F_8N_{10}Ru$

Compounds referred to in this dataset (continued)

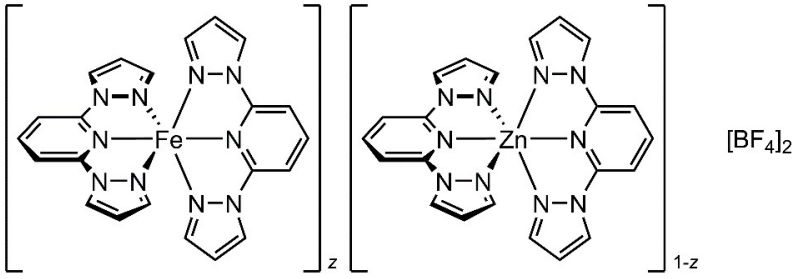

$[Fe_zZn_{1-z}(bpp)_2][BF_4]_2$
Bis[di(pyrazol-1-yl)pyridine]iron(II):zinc di(tetrafluoroborate) solid solution
$C_{22}H_{18}B_2F_8Fe_zN_{10}Zn_{1-z}$
z = 0.89, **1a**
z = 0.69, **1b**
z = 0.51, **1c**
z = 0.26, **1d**
z = 0.07, **1e**

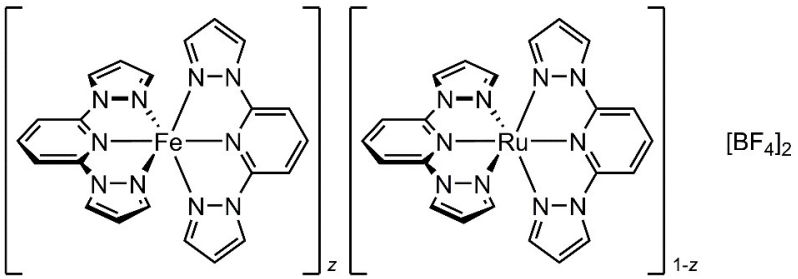

$[Fe_zRu_{1-z}(bpp)_2][BF_4]_2$
Bis[di(pyrazol-1-yl)pyridine]iron(II):ruthenium di(tetrafluoroborate) solid solution
$C_{22}H_{18}B_2F_8Fe_zN_{10}Ru_{1-z}$
z = 0.88, **2a**
z = 0.67, **2b**
z = 0.49, **2c**
z = 0.14, **2d**

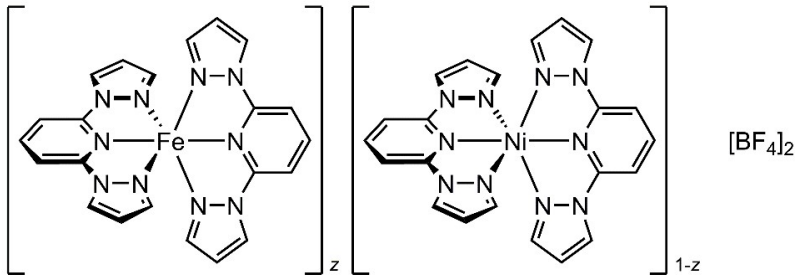

$[Fe_zNi_{1-z}(bpp)_2][BF_4]_2$
Bis[di(pyrazol-1-yl)pyridine]iron(II):nickel di(tetrafluoroborate) solid solution
$C_{22}H_{18}B_2F_8Fe_zN_{10}Ni_{1-z}$
z = 0.50, **3c**

Compounds referred to in this dataset (continued)

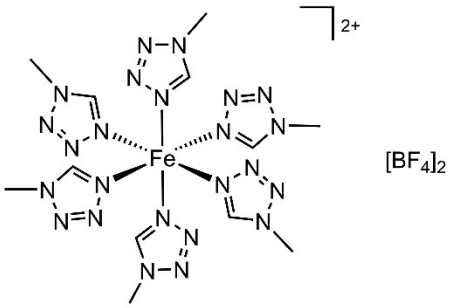

$[Fe(mtz)_6][BF_4]_2$
Hexakis[1-methyltetrazole]iron(II) di(tetrafluoroborate)
$C_{12}H_{24}B_2F_8FeN_{24}$

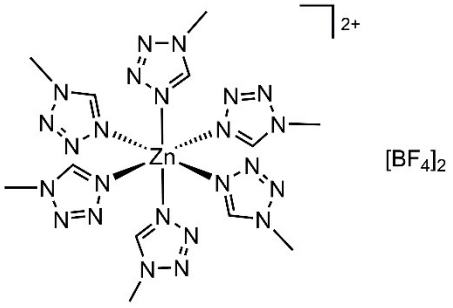

$[Zn(mtz)_6][BF_4]_2$
Hexakis[1-methyltetrazole]zinc(II) di(tetrafluoroborate)
$C_{12}H_{24}B_2F_8N_{24}Zn$

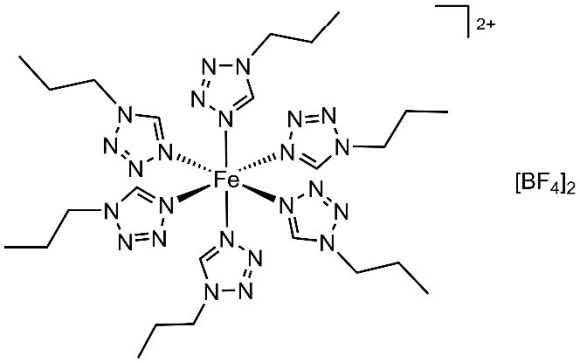

$[Fe(ptz)_6][BF_4]_2$
Hexakis[1-propyltetrazole]iron(II) di(tetrafluoroborate)
$C_{24}H_{48}B_2F_8FeN_{24}$

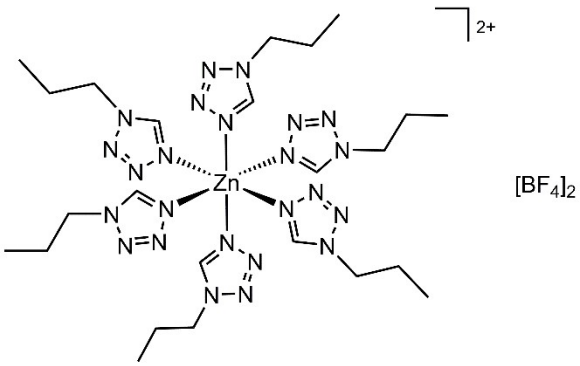

$[Zn(ptz)_6][BF_4]_2$
Hexakis[1-propyltetrazole]zinc(II) di(tetrafluoroborate)
$C_{24}H_{48}B_2F_8N_{24}Zn$

Compounds referred to in this dataset (continued)

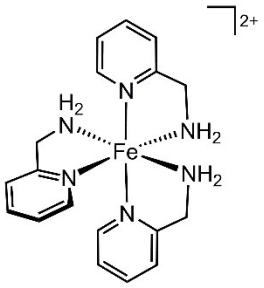

$Cl_2 \cdot EtOH$

$[Fe(pic)_3]Cl_2 \cdot EtOH$
Tris[2-(aminomethyl)pyridine]iron(II) dichloride ethanol solvate
$C_{20}H_{30}Cl_2FeN_6O$

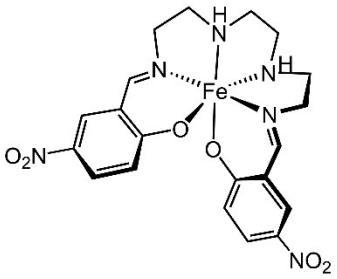

$[Fe(5\text{-}\{NO_2\}_2\text{-saltrien})_2]$
[5-Nitrosalicylaldehyde-1,4,7,10-tetraazadecane]iron(II)
$C_{20}H_{22}FeN_6O_6$

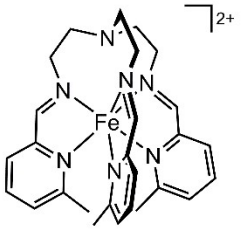

$[ClO_4]_2$

$[Fe(\{MePy\}_3tren)][ClO_4]_2$
[Tris-({6-methylpyrid-2-yl}-3-aza-3-butenyl)amine]iron(II) diperchlorate
$C_{27}H_{33}Cl_2FeN_7O_8$

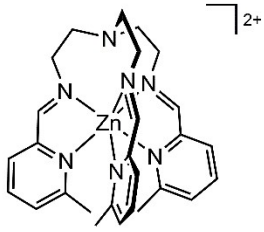

$[ClO_4]_2$

$[Zn(\{MePy\}_3tren)][ClO_4]_2$
[Tris-({6-methylpyrid-2-yl}-3-aza-3-butenyl)amine]zinc(II) diperchlorate
$C_{27}H_{33}Cl_2N_7O_8Zn$

Compounds referred to in this dataset (continued)

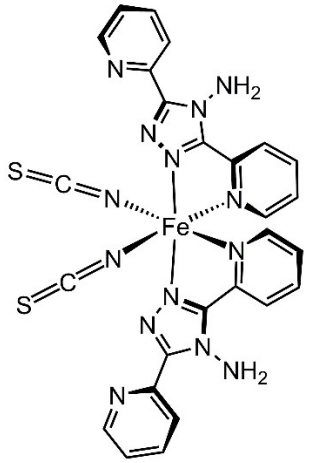

$[Fe(NCS)_2(abpt)_2]$
Bis[4-amino-3,5-bis(pyridin-2-yl)-1,2,4-triazole]di(isothiocyanato)iron(II)
$C_{26}H_{20}FeN_{14}S_2$

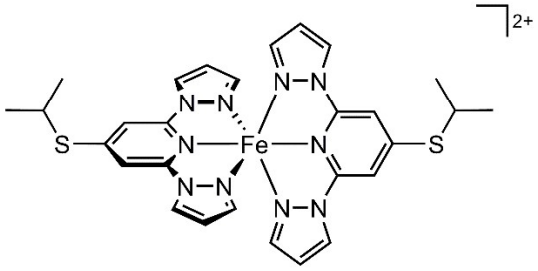

$[BF_4]_2 \cdot MeCN$

$[Fe(bpp^{SiPr})_2][BF_4]_2 \cdot MeCN$
Bis[4-(*iso*propylsulfanyl)-2,6-di(pyrazol-1-yl)pyridine]iron(II) ditetrafluoroborate acetonitrile solvate
$C_{30}H_{33}B_2F_8FeN_{11}S_2$

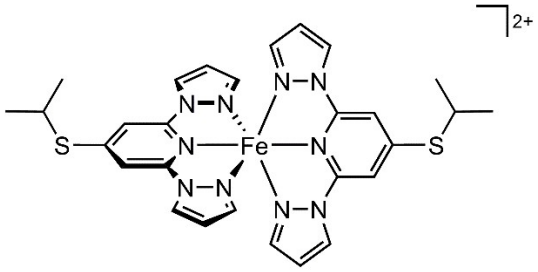

$[BF_4]_2 \cdot MeNO_2$

$[Fe(bpp^{SiPr})_2][BF_4]_2 \cdot MeNO_2$
Bis[4-(*iso*propylsulfanyl)-2,6-di(pyrazol-1-yl)pyridine]iron(II) ditetrafluoroborate nitromethane solvate
$C_{29}H_{33}B_2F_8FeN_{11}O_2S_2$